

3.3 Semi-Inclusive DIS

Semi-inclusive deep inelastic scattering (SIDIS) has been used extensively in recent years as an important testing ground for QCD. Studies so far have concentrated on better determination of parton distribution functions, distinguishing between the quark and antiquark contributions, and understanding the fragmentation of quarks into hadrons. The use of polarization in lepton production provides an essential new dimension for testing QCD.

Spin and azimuthal asymmetries in distributions of final state particles in deep inelastic scattering (DIS) play a crucial role in the study of the spin structure of hadrons in terms of their elementary constituents [19, 96, 20, 21, 25]. In particular measurement of the azimuthal angle dependence of the observed hadron allows access to various transverse momentum dependent (TMD) distributions [17, 18, 19, 20, 21, 23] containing direct information about the quark orbital motion [26, 25, 28].

It is also argued that in both semi-inclusive [97] and in hard exclusive [98, 53, 99] pion production, scaling sets in for cross section ratios and, in particular, for spin asymmetries at lower Q^2 than it does for the absolute cross section. The very good agreement of the HERMES data with the SMC data, taken at 6-12 times higher average Q^2 , shows that the semi-inclusive asymmetries are Q^2 independent within the present accuracy of the experiments [100]. This makes it possible for the measurement of spin-asymmetries to be a major tool for the study of different parton distribution function (TMD,GPD) measurements in the Q^2 domain of a few GeV^2 .

The total cross section for single pion production by longitudinally polarized leptons scattering off unpolarized protons is defined by a set of structure functions and contains two main contributions. The beam spin-independent part of the cross section (σ_{UU} in Ref. [20]) arises from the symmetric part of the hadronic tensor, and the helicity (λ_e) dependent part (σ_{LU})[96] arises from the antisymmetric part:

$$\begin{aligned} \frac{d\sigma_{UU}}{dx_B dy dz d^2 P_\perp} &= \frac{4\pi \alpha^2 s}{Q^4} x_B \left\{ \left(1 - y + \frac{1}{2} y^2 + \frac{1}{4} \gamma^2\right) \mathcal{H}_T + \left(1 - y - \frac{1}{4} \gamma^2\right) \mathcal{H}_L \right. \\ &\quad \left. - (2 - y) \sqrt{1 - y - \frac{1}{4} \gamma^2} \cos \phi \mathcal{H}_{LT} + \left(1 - y - \frac{1}{4} \gamma^2\right) \cos 2\phi \mathcal{H}_{TT} \right\}, \\ \frac{d\sigma_{LU}}{dx_B dy dz d^2 P_\perp} &= \lambda_e \frac{4\pi \alpha^2 s}{Q^4} x_B \sqrt{y^2 + \gamma^2} \sqrt{1 - y - \frac{1}{4} \gamma^2} \sin \phi \mathcal{H}'_{LT}, \end{aligned} \quad (3.31)$$

where ϕ is the azimuthal angle between the scattering plane formed by the initial (k_1) and final (k_2) momenta of the electron and the production plane formed by the transverse momentum of the observed hadron (P_\perp) and the virtual photon (see Fig.3.30). The target mass corrections are explicitly included in the kinematics via the term $\gamma^2 = 4M^2 x_B^2 / Q^2$.

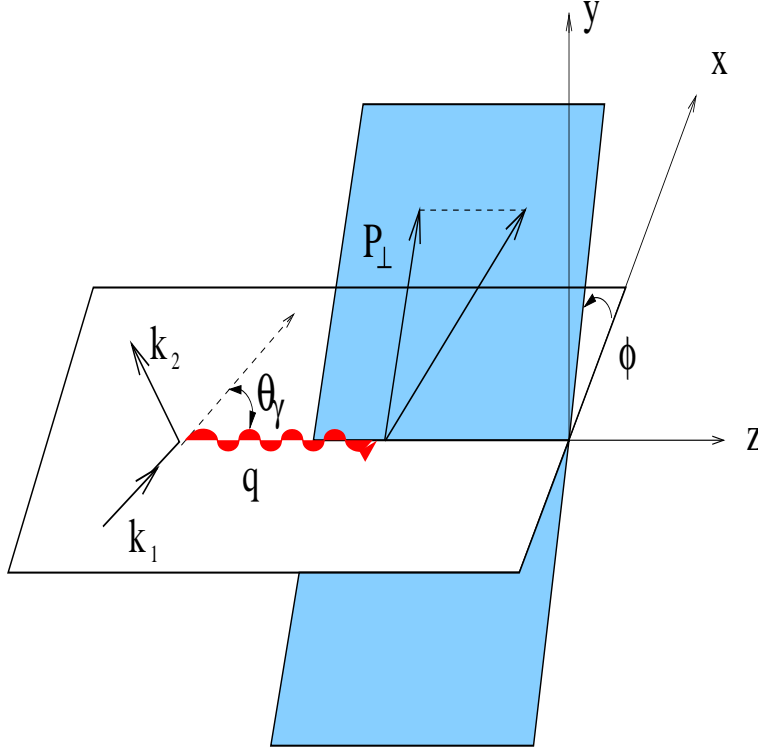


Figure 3.30: Kinematics for the pion electroproduction.

The relevant kinematical variables are defined as: $x_B = Q^2/2P_1 \cdot q$, $y = P_1 q/P_1 \cdot k_1$, $z = P_1 \cdot P/P_1 \cdot q$, where $Q^2 = -q^2$, $q = k_1 - k_2$ is the momentum of the virtual photon, and P_1 and P are the target and observed final-state hadron momenta, respectively.

The structure functions \mathcal{H}_T , \mathcal{H}_L , \mathcal{H}_{TT} , \mathcal{H}_{LT} , and $\mathcal{H}_{LT'}$ are related to the transverse and longitudinal photon contributions and their interference. Additional single and double spin-dependent contributions with corresponding structure functions appear in the SIDIS cross section for polarized targets or if one considers polarimetry in the final state. Assuming that the quark scattering process and the fragmentation process factorize, and that the fragmentation functions scale and depend only on the fractional energy, z , the structure functions could be presented as a convolution of a distribution function and a fragmentation function. Both assumptions have yet to be experimentally confirmed at JLab energies.

At the leading-twist level, the quark structure of hadrons is described by three distribution functions: the number density, or unpolarized distribution function, $q(x)$; the helicity distribution, $\Delta q(x)$; and the transversity distribution, $\delta q(x)$. If the transverse momentum k_T of partons also included, the number of independent distribution functions at leading twist increases to six [20, 21, 24] (three of which reduce to $q(x)$, $\Delta q(x)$ and $\delta q(x)$ when integrated over k_T). Because they in general depend on the longitudinal and transverse momentum, these “3-dimensional” TMD functions

distribution functions		chirality	
		even	odd
twist 2	U	q	h_1^\perp
	L	$\Delta\mathbf{q}$	h_{1L}^\perp
	T	f_{1T}^\perp g_{1T}	$\delta\mathbf{q}$ h_{1T}^\perp
twist 3	U	f^\perp	e
	L	g_L^\perp	\mathbf{h}_L
	T	\mathbf{g}_T g_T^\perp	h_T h_T^\perp

Table 3.1: List of twist-2 and twist-3 distribution functions accessible in SIDIS.

provide a more complete picture of nucleon structure. Relaxing the time invariance condition, two additional functions (f_{1T}^\perp, h_1^\perp) are permitted [18, 22, 101, 25, 26, 23], bringing the total number of distribution functions to eight.

With better experimental accuracy it may be possible to isolate the higher-twist effects in hard processes, which arise from the quantum mechanical interference of partons in the interacting hadrons. The higher-twist terms are important for understanding long-range quark-gluon dynamics and may be accessible through measurements of certain asymmetries[30, 96, 21, 20], where they appear as leading contributions. Higher-twist structure functions are important at CEBAF energies because of the phenomenon of parton-hadron duality [61], or ‘precocious scaling’ [76, 91]. The full list of twist-2 and twist-3 distribution functions (those that survive after the k_T -integration are denoted in boldface) contributing to the double-polarized cross section in SIDIS is shown in Table 3.1 (see [20]):

Parton distribution functions cannot be computed in perturbative QCD. They are universal and do not depend on the particular hard process. Once measured in SIDIS no extra input is needed in order to compute analogous quantities in hadron-hadron collisions. Until recently the TMD distribution functions had mainly academic interest. They appear in azimuthal moments of double-polarized cross sections in single-hadron production in DIS [20, 21]. As shown recently in Ref.[23], the interaction of active parton in the hadron and the target spectators lead to gauge-invariant TMD parton distributions in DIS. Brodsky et al. [25] discussed final state diffractive scattering, which gives rise to interference effects in the DIS cross section[102]. A non trivial phase structure of QCD amplitudes due to rescattering results in *time-reversal odd* (T-odd) effects and the appearance of single-spin asymmetries at leading twist[25, 26]. This opens up a unique possibility to access T-odd distribution functions in single-spin asymmetry measurements in semi-inclusive DIS [25, 26].

A major issue in studies of semi-inclusive scattering is the separation of contributions from current fragmentation (active parton) and target fragmentation (spectators). It was argued [103] that, within perturbative QCD, it is possible to introduce new universal functions, so-called “fracture functions”, describing the target hadron

once it has fragmented into a specific final state hadron. These fracture functions depend on the initial and final hadrons, as well as on the quark flavor, and are functions of two momentum fractions, Bjorken x_B and the Feynman z variable.

A key goal is to carefully study the transition between the nonperturbative and perturbative regimes of QCD using simultaneous measurements of the Q^2 and x_B dependencies of cross sections and beam/target spin asymmetries for different final state hadrons with extraction of the corresponding structure functions and separation of the contributions of different distribution and fragmentation functions.

3.3.1 Single-Spin Asymmetries

Single-spin asymmetries (SSA) in hadronic reactions have been among the most difficult phenomena to understand from first principles in QCD. Large SSAs have been observed in hadronic reactions for decades [104, 105]. Recently, significant SSAs were reported in SIDIS by the HERMES collaboration at HERA [106, 107] (for a longitudinally polarized target), the SMC collaboration at CERN (transversely polarized targets) [108], and the CLAS collaboration at JLab[16] (polarized beam). In general, such single-spin asymmetries require a correlation of a particle spin with a production or scattering plane. In hadronic processes, such correlations can provide a window to the physics of final and initial state interactions.

Single-spin asymmetries in SIDIS give access to subtle distribution and fragmentation functions, which cannot easily be accessed in other ways. The list of novel physics observables accessible in SSAs includes the chiral-odd distribution functions, such as the transversity (δq) [30], the *time-reversal odd* fragmentation functions, in particular the Collins function (H_1^\perp) [19], and the recently introduced [18, 22, 25, 26, 28] *time-reversal odd* distribution functions (f_{1T}^\perp, h_1^\perp). These latter functions arise from interference between amplitudes with left- and right-handed polarization states, and only exist because of chiral symmetry breaking in QCD. Their study therefore provides a new avenue for probing the chiral nature of the partonic structure of hadrons. Furthermore, it was demonstrated recently that a nonzero orbital angular momentum of partons in the nucleon is crucial in forming the target SSA. The interference of different amplitudes arising from the target hadron's wavefunction that gives single-spin asymmetries [25], also yields the Pauli form factor $F_2(t)$ and the GPD $E(x, \xi, t)$ [109, 24] entering Deeply Virtual Compton Scattering[110, 111].

Unpolarized target

Assuming factorization of the quark scattering and fragmentation processes, the distribution and fragmentation functions responsible for a non-zero \mathcal{H}'_{LT} in SIDIS were first identified by Levelt and Mulders [96]. They include the twist-3 unpolarized distribution function $e(x)$ introduced by Jaffe and Ji [30], and the polarized fragmentation function $H_1^\perp(z)$ first discussed by Collins [19]. The first ever extraction of

the twist-3 distribution function from CLAS data [112] is shown in Fig.3.31. With a certain approximation for the twist-3 function $e(x)$, the beam SSA could become a major source of information on the T-odd polarized fragmentation function.

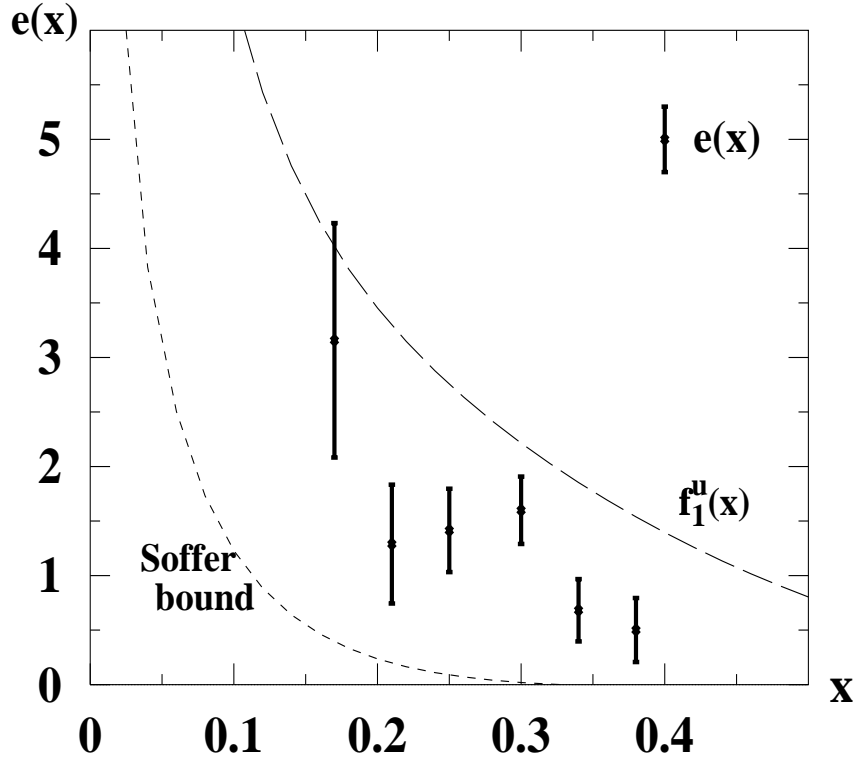


Figure 3.31: The flavor combination $e(x) = (e^u + \frac{1}{4}e^{\bar{d}})(x)$ vs. x , extracted from the CLAS beam-spin azimuthal asymmetry. The error bars are due to statistical errors of the CLAS data with $\langle Q^2 \rangle = 1.5 \text{ GeV}^2$. A fit to published HERMES data[106] on target SSA was used in the parameterization of the Collins function. For comparison $u(x)(f_1^u(x))$ and the twist-3 Soffer bound are shown.

Beam SSAs do not require polarized targets and are free of dilution. They could be measured at the highest accessible luminosities. This makes them an important tool for factorization studies using measurements of different final state hadrons.

Polarized targets

For polarized targets, several azimuthal asymmetries already arise at leading order. The following contributions were investigated in Refs. [19, 20, 21, 113, 25, 28]:

$$\sigma_{LT}^{\cos\phi} \propto \lambda_e S_T y (1 - y/2) \cos(\phi - \phi_S) \sum_{q,\bar{q}} e_q^2 x g_{1T}^q(x) D_1^q(z), \quad (3.32)$$

$$\sigma_{UL}^{\sin 2\phi} \propto S_L 2(1 - y) \sin 2\phi \sum_{q,\bar{q}} e_q^2 x h_{1L}^{\perp q}(x) H_1^{\perp q}(z), \quad (3.33)$$

$$\begin{aligned} \sigma_{UT}^{\sin\phi} &\propto S_T (1 - y) \sin(\phi - \phi_S) \sum_{q,\bar{q}} e_q^2 x \delta q(x) H_1^{\perp q}(z), \\ &+ S_T (1 - y + y^2/2) \sin(\phi + \phi_S) \sum_{q,\bar{q}} e_q^2 x f_{1T}^{\perp q}(x) D_1^q(z), \end{aligned} \quad (3.34)$$

where ϕ_S is the azimuthal angle of the transverse spin in the photon frame and $D_1^q(z)$ is the spin-independent fragmentation function. The subscripts “U, L, T” in $\sigma_{BT}^{W(\phi)}$ ($W(\phi) = \sin\phi, \cos\phi, \sin 2\phi$) stand for the unpolarized “U”, longitudinally polarized “L”, and transversely polarized “T” states of the beam (first index) and target (second index). Corresponding moments can be measured as

$$A_{BT}^W = \int \sigma_{BT}(\phi) W(\phi) d\phi / \int \sigma(\phi) d\phi.$$

The latter two equations above describe single-spin asymmetries involving the first moment of the Collins fragmentation function integrated over the transverse momentum of the final hadron. The leading-twist SSA $\sigma_{UL}^{\sin 2\phi}$ is kinematically suppressed at low x_B compared to the sub-leading $\sin\phi$ moment [114]. A recent measurement of the σ_{UL} contribution by HERMES[106] is consistent with a zero $\sin 2\phi$ moment. However, at the large x_B values accessible at JLab, the $A_{UL}^{\sin 2\phi}$ asymmetry is predicted [114] to be large (see Fig.3.32). The leading-twist distribution function $h_{1L}^{\perp}(x)$, accessible in that measurement, describes the transverse polarization of quarks in a longitudinally polarized proton.

The $\sin\phi$ moment of the SIDIS cross section with a transversely polarized target (σ_{UT})[101] contains contributions both from the Sivers effect (T-odd distribution)[18] and the Collins effect (T-odd fragmentation)[19]. Contributions to transverse SSAs from T-odd distributions of initial quarks ($f_{1T}^{\perp q}(x)$ term) and T-odd fragmentation of final quarks ($H_1^{\perp q}(z)$ term) could be separated by their different azimuthal and z -dependencies.

Assuming that the transversity of the sea is negligible ($\delta\bar{q} = 0$) and ignoring the non-valence quark contributions in pion production, the single-spin transverse asymmetry arising from fragmentation becomes:

$$A_{UT}^{\pi^+} \propto \frac{4\delta u(x)}{4u(x) + \bar{d}(x)} \frac{H_1^{\perp u \rightarrow \pi^+}(z, P_{\perp})}{D_1^{u \rightarrow \pi^+}(z, P_{\perp})}, \quad (3.35)$$

$$A_{UT}^{\pi^-} \propto \frac{\delta d(x)}{d(x) + 4\bar{u}(x)} \frac{H_1^{\perp d \rightarrow \pi^-}(z, P_{\perp})}{D_1^{d \rightarrow \pi^-}(z, P_{\perp})}, \quad (3.36)$$

$$A_{UT}^{\pi^0} \propto \frac{4\delta u(x) + \delta d(x)}{4u(x) + \bar{d}(x) + d(x) + 4\bar{u}(x)} \frac{H_1^{\perp d \rightarrow \pi^0}(z, P_{\perp})}{D_1^{d \rightarrow \pi^0}(z, P_{\perp})}. \quad (3.37)$$

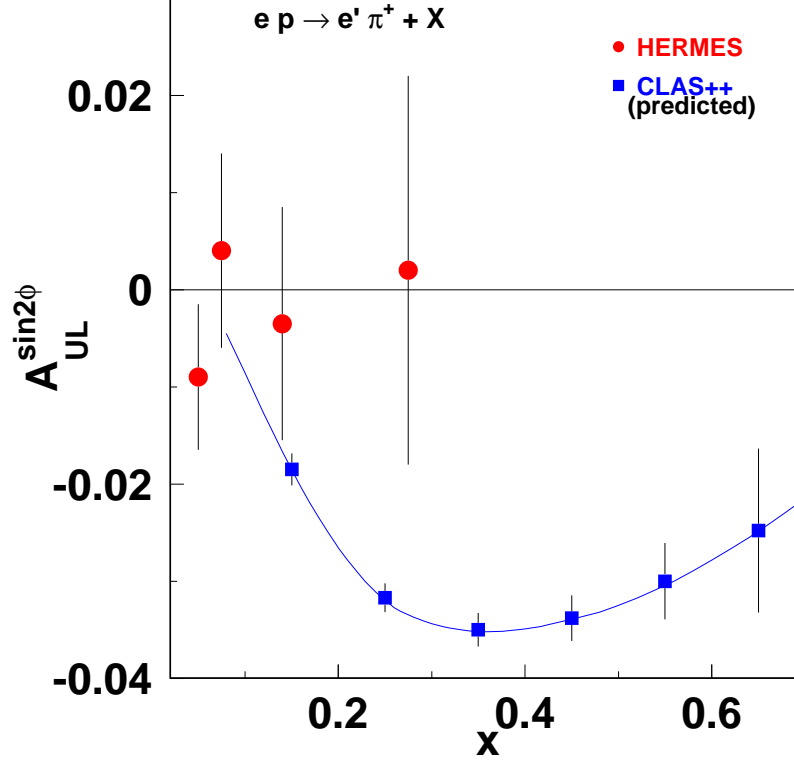


Figure 3.32: Dependence on x of longitudinally polarized target SSA, $A_{UL}^{\sin 2\phi}$. Circles are HERMES data for $A_{UL}^{\sin 2\phi}$, and squares represent expected statistical errors from CLAS at 11 GeV with 2000 hours of data taking. The curve is the prediction from Ref.[114].

The target single-spin asymmetry from polarized quark fragmentation extracted for CLAS kinematics at 12 GeV is plotted in Fig. 3.33. The estimate was done assuming $\delta q \approx \Delta q$ and an approximation for the Collins fragmentation function from Ref.[114]. Additional cuts were applied on z ($z > 0.5$) and the missing mass of the $e' \pi^+$ system ($M_X(\pi^+) > 1.1$ GeV). The curves have been calculated assuming a luminosity of $10^{35} \text{cm}^{-2} \text{s}^{-1}$, with a NH^3 target polarization of 85% and a dilution factor 0.176, with 2000 hours of data taking. The asymmetry is integrated over all hadron transverse momenta. The extraction of the transversity from $A_{UT}^{\sin \phi}$ could be performed via Eqs. (3.35-3.37) using parameterizations for the unpolarized distribution functions $u(x)$ and $\bar{d}(x)$.

The SIDIS cross section with a longitudinally polarized target in the sub-leading order contains an additional contribution to the $\sin \phi$ moment (σ_{UL}) [113, 101, 115]:

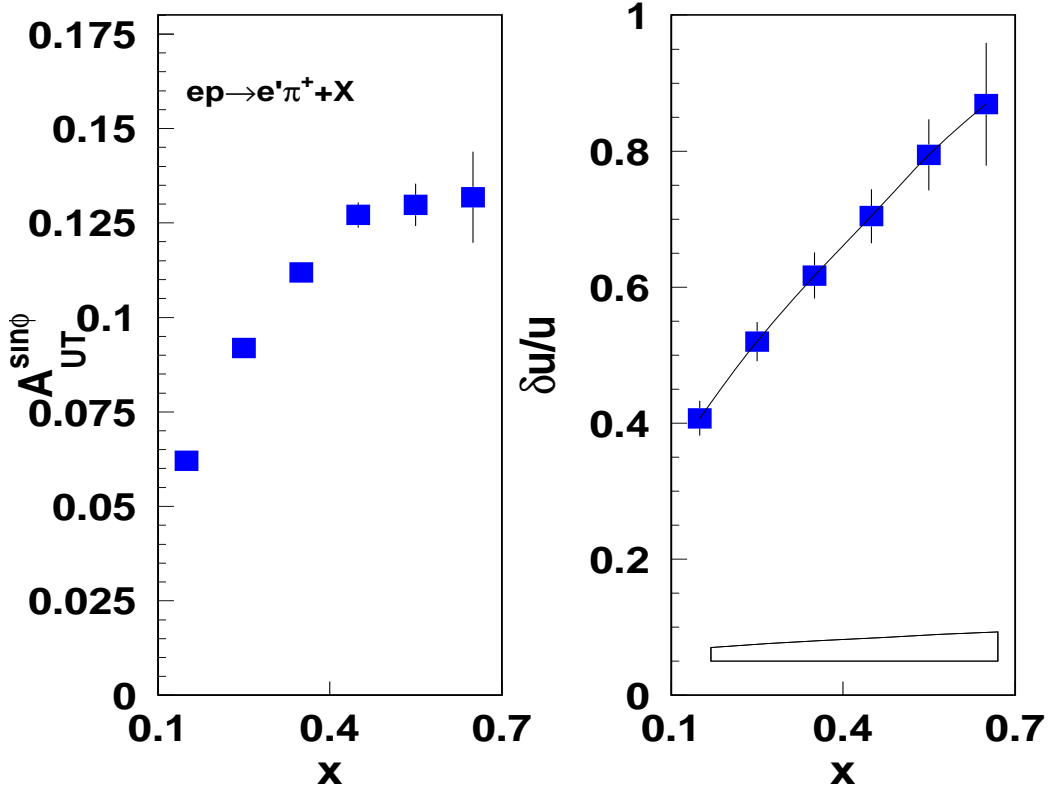


Figure 3.33: Projected transverse spin asymmetry ($A_{UT}^{\sin\phi}$) in single π^+ production with CLAS at 12 GeV (left plot) and the expected precision of the extracted $\delta u/u$ (right plot). The line is the Monte Carlo generated $\delta u/u$ and the band represent uncertainty due to unknown fragmentation function.

$$\sigma_{UL}^{\sin\phi} \propto S_L \sin\phi (2-y) \sqrt{1-y} \frac{M}{Q} \sum_{q,\bar{q}} e_q^2 x^2 h_L^q(x) H_1^{\perp q}(z). \quad (3.38)$$

The $\sin\phi$ moment of the cross section measured at CLAS is in good agreement with the HERMES measurement, which indicates that the asymmetry observables are not sensitive to the beam energy (see Fig.3.34). There are several different approaches[53, 116, 25] to the interpretation of the sign flip of the target SSA at large z observed by HERMES[106], and more data are needed to separate the different contributions.

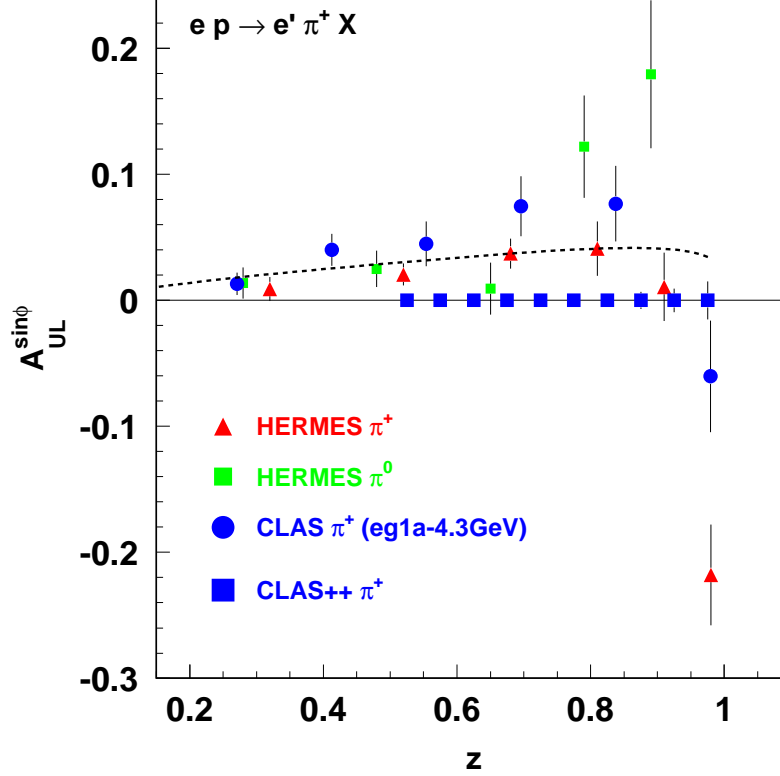


Figure 3.34: $A_{UL}^{\sin\phi}$ as a function of z from CLAS compared to HERMES [106, 107]. Squares are projection of CLAS 12 GeV. The curve is the prediction from [115] for HERMES kinematics.

3.3.2 Flavor Decomposition

The SIDIS cross section for a polarized beam and a polarized target contains contributions σ_{LT} and σ_{LL} proportional to the beam helicity (λ_e) and the transverse (S_T) and longitudinal (S_L) components of the target spin with respect to the virtual photon direction [20]. The most well-known result for leptonproduction is the double-polarized asymmetry integrated over the final hadron transverse momentum:

$$\sigma_{LL} \propto \lambda_e S_L y (1 - y/2) \sum_{q,\bar{q}} e_q^2 x \Delta q(x) D_1^q(z).$$

The semi-inclusive double-polarization asymmetries with a longitudinally polarized target (σ_{LL}) have been the subject of considerable interest recently, both theoretically and experimentally. On the experimental side, luminosity has been one of the main constraints limiting measurements beyond $x = 0.5$. While the polarized u -quark

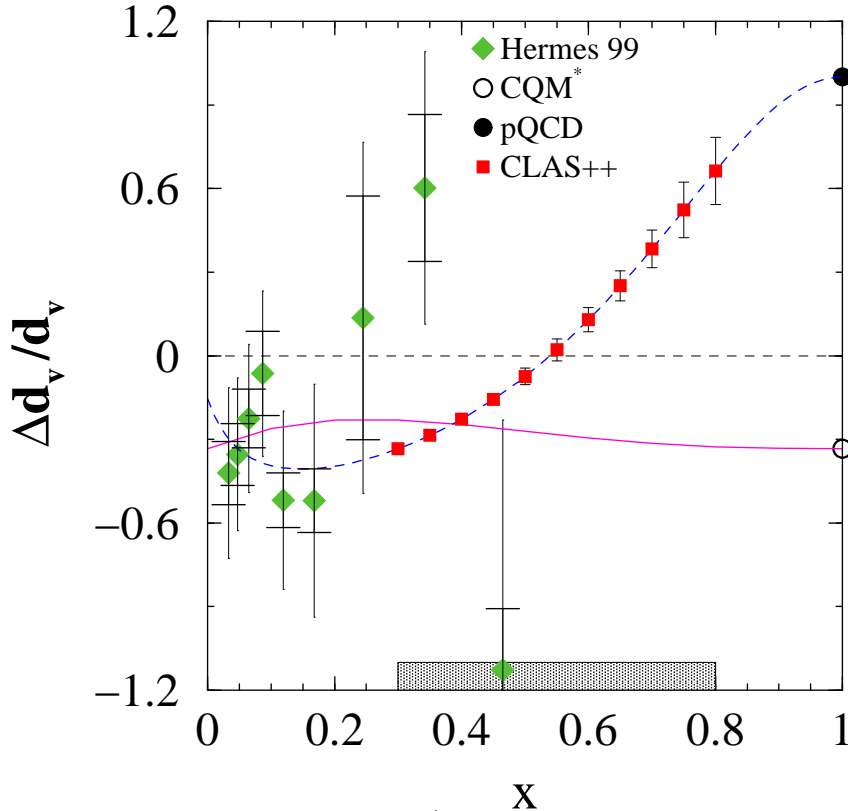


Figure 3.35: Projection of CLAS $\Delta d/d$ measurements at large x , compared with the constituent quark model (CQM) and pQCD-based parameterizations.

distribution is reasonably well established experimentally, the polarized d -quark distribution is poorly known, especially at large x , where there are significant differences between predictions derived from non-perturbative and perturbative models of QCD. The data shown in Fig. 3.35 represent the present knowledge of Δd at large x . An energy and luminosity upgraded CLAS will allow measurements in the x region above 0.5. Assuming factorization, SIDIS measurements may be used to extract polarized distribution functions using polarized proton and deuteron targets. The extraction of polarized-quark distribution functions from semi-inclusive asymmetries could be done either using the purity technique [100] or the method based on the extraction of spin asymmetries in the difference of π^+ and π^- counts [117].

3.3.3 Semi-Exclusive Meson Production

In the processes of semi-exclusive electroproduction, the final meson is produced at short distances via hard-gluon exchange [118, 119, 120], with a characteristic rapidity gap between the current fragmentation region and target fragmentation region. This mechanism is expected to dominate the cross section in the kinematic regime where

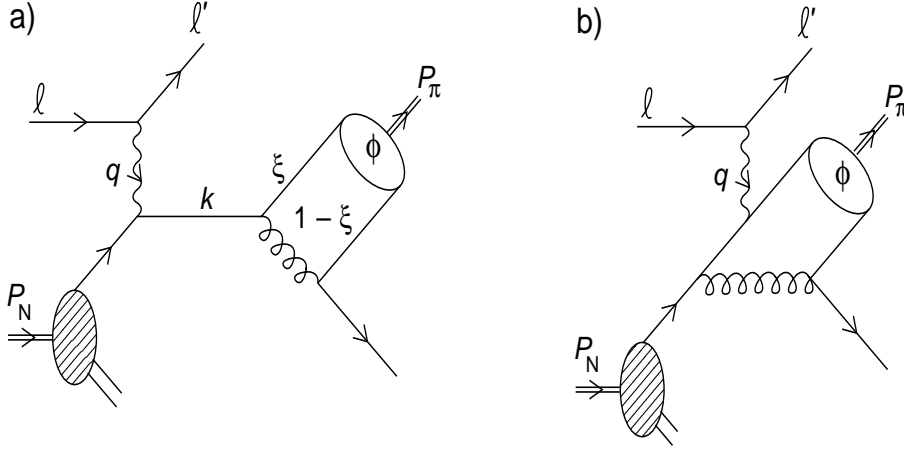


Figure 3.36: Leading contributions to the amplitude of the reaction $u + e^- \rightarrow e^- + \pi^+ + d$.

the ejected meson picks up most of the virtual photon momentum (or large z) [119]. Phenomenological fragmentation functions are not required to describe this important class of deep-inelastic processes, since the mechanism of meson production from a quark is described exactly by pQCD. One can view it as a first step in solving the problem of meson formation in hard processes. It is essential that in the theory of semi-exclusive reactions, formation of the final hadronic state is described in terms of quark distribution amplitudes, therefore providing a connection between inclusive and exclusive reactions (see Fig. 3.36). It was also noted that with CEBAF upgraded to 12 GeV, the semi-exclusive channel allows one to reach high virtuality of the exchanged gluon, corresponding to about $Q^2 \sim 30 \text{ GeV}^2$ for the exclusive case of the pion form factor [121].

It was shown in Ref.[118] that higher twist effects may be isolated in semi-exclusive pion production for moderate values of Q^2 . Significant $\cos \phi$ and $\cos 2\phi$ moments (see Fig.3.37) were predicted in the exclusive limit ($z \rightarrow 1$).

An important physics implication of connection between inclusive and exclusive reactions is that the corresponding subprocess, $\gamma^* q \rightarrow \pi q$, is an essential component of the formalism of Deeply Virtual Meson production. Semi-inclusive measurements may therefore produce model-independent information necessary to extract (polarized) Generalized Parton Distributions from deeply-virtual exclusive electroproduction of mesons.

The CLAS⁺⁺ detector can provide complete kinematic coverage of semi-exclusive electroproduction reactions in the deep-inelastic region.

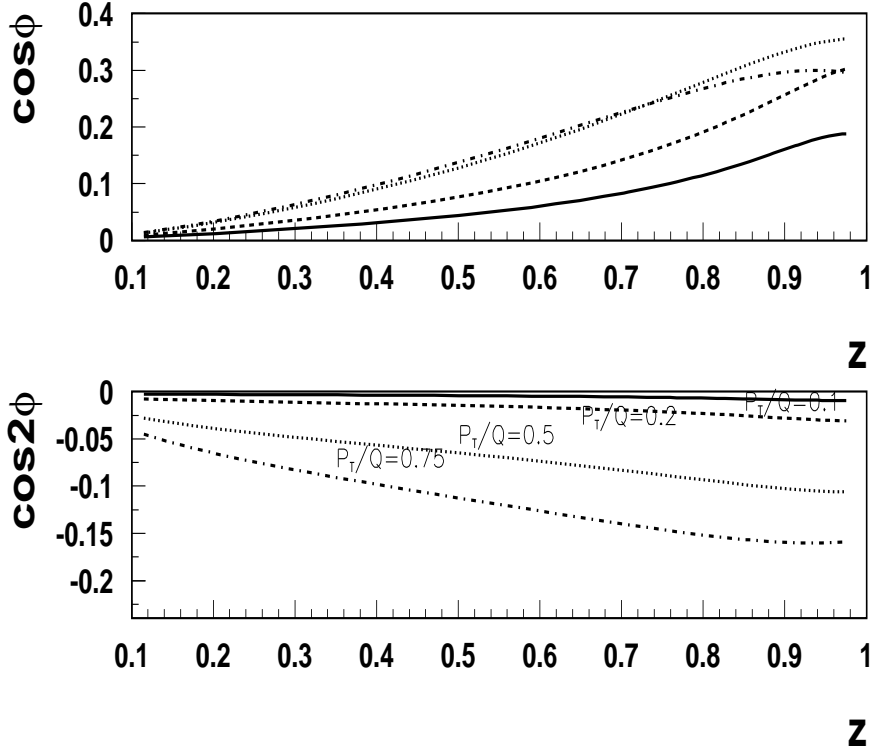


Figure 3.37: Azimuthal moments in unpolarized cross section as a function of z for different values of transverse momentum of the final π^+ .

3.3.4 Conclusions

In summary, with upgraded energy and luminosity, CLAS can study single- and double-spin asymmetries, involving essentially unexplored chiral-odd and time-odd distribution functions, like transversity[29, 30], Sivers[18, 25, 26, 28] and Collins[19] functions and shed light on the quark transverse momentum distributions and the orbital angular momentum [19, 21, 20, 109, 122]. With good particle identification, single- and double-spin asymmetries can be extracted for different hadrons, enabling flavor decomposition of different distribution functions. Measurement of SSAs with K^+ (see Fig. 3.38 for the ratio of K^+ , π^+ yields) in comparison with SSA for π^+ would provide an experimental test of factorization and u -quark dominance at JLab energies[123].

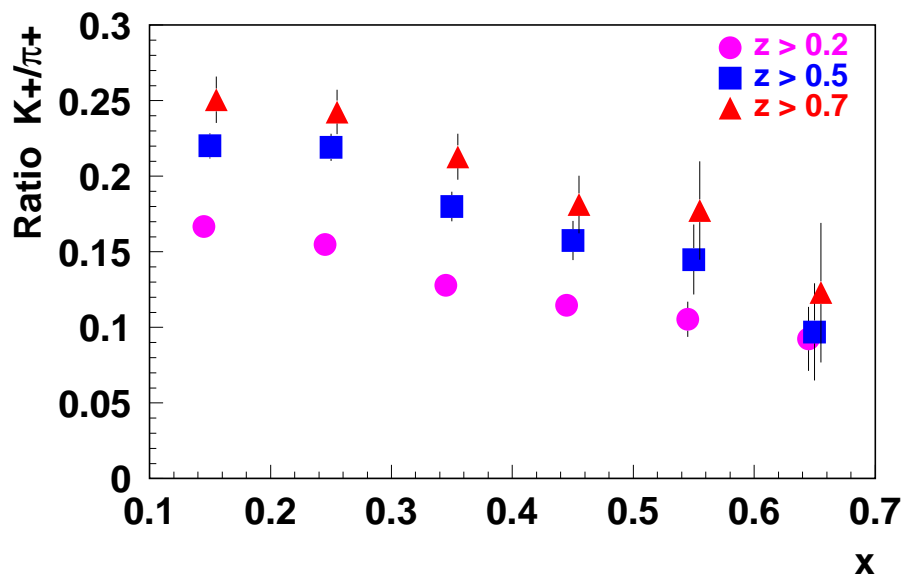


Figure 3.38: The expected ratio of K^+ to π^+ as a function of x_B from CLAS with 12 GeV, based on studies from the LEPTO event generator.